Available online at www.sciencedirect.com
ScienceDirect
International Journal of Coal Geology 71 (2007) 329–344
International Journal of COAL GEOLOGY
www.elsevier.com/locate/ijcoalgeo

REE Geochemistry of the Cretaceous lignite from Wulantuga Germanium Deposit, Inner Mongolia, Northeastern China

Huawen Qi [a,*], Ruizhong Hu [a], Qi Zhang [a,b]

[a] *State Key laboratory of Ore Deposit Geochemistry, Institute of Geochemistry, Chinese Academy of Sciences, Guiyang 550002, China*
[b] *Graduate School, Chinese Academy of Sciences, Beijing 100039, China*

Received 4 August 2006; received in revised form 22 November 2006; accepted 11 December 2006
Available online 20 December 2006

Abstract

The Wulantuga Germanium Deposit (WGD), hosted in coal seams with Ge resources up to 1600 Mt, is located in the Shengli Coalfield in Xilingol, Inner Mongolia, China. Forty-two channel samples of Ge-bearing lignites of the No. 6-1 coal seam (Lower Cretaceous Bayanhua Formation) were collected and their REE compositions were analyzed by inductively coupled plasma mass spectrometry (ICP-MS). The modes of occurrence of REE in selected lignite samples were studied by scanning electron microscope with energy-dispersive X-ray spectrometer (SEM-EDX) and statistical methods. The distribution of REE and Y in all 42 samples from WGD are in accordance with the log normal distribution, the total rare earth element content (∑REE) of most lignite samples from WGD range from 9.02 to 118 ppm, only four samples show relatively higher (149–533 ppm) ∑REE concentration. The average REE contents of 42 lignite samples from WGD are slightly higher than those of the USA coals, world wide coals, sandstone from WGD, and the contemporary Ge-barren lignite from Hongqi Coal Mine. The lignite samples from WGD have shale-like Chondrite or NASC-normalized REE patterns similar to those of sandstone overburden and Ge-barren lignite from Hongqi Coal Mine. REE contents of most lignite samples are highly positive correlated with ash yields, indicating a mainly detrital source and association with syngenetic mineral matter. REE-rich phosphates (monazite) were identified by SEM-EDX in some medium-to high-ash (ash yields range from 23.58% to 38.18%) lignite samples with high ∑REE+Y contents from WGD. REE can be concentrated in the upper and lower proportions of the No. 6-1 coal seam. The vertical profiles of REE mainly follow that of TiO_2, and the average REE/TiO_2 ratio of lignite sample in three sections is very close to that of the sandstone from WGD or lignite from Hongqi Coal Mine. It was determined that most REE in the lignite from WGD were derived from a detrital source and associated with syngenetic mineral matter. However, when normalized to the overlying sandstone, some lignite samples from WGD display a small but distinct enrichment in middle-to heavy-REE, indicating small quantity of middle-to heavy-REE may be added and/or retained during epigenesis. The lignite samples from WGD are characterized by higher ratios of LREE/HREE and Eu/Eu*, and horizontal NASC-normalized REE patterns, and distinguished from those of the Ge-bearing lignites from Lincang Germanium Deposit, Yunnan, China and Ge deposits of Russian Far East. There is no distinct correlations between Ge and any individual REE or ∑REE+Y content of lignite from WGD.

Keywords: Lignite; REE; Wulantuga Germanium Deposit; Inner Mongolia; China

1. Introduction

The main factors for the concentration of the Rare earth elements (REE) and Y in coal are the source area

* Corresponding author. Fax: +86 851 589 1664.
E-mail address: qihuawen@vip.gyig.ac.cn (H. Qi).

0166-5162/$ - see front matter © 2006 Elsevier B.V. All rights reserved.
doi:10.1016/j.coal.2006.12.004

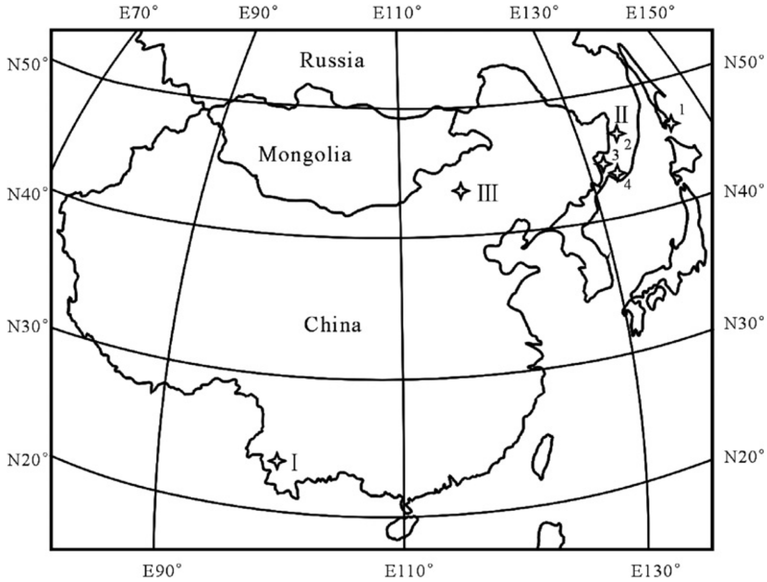

Fig. 1. Locations of coal hosted large germanium deposits (Ge reserve > 1000 MT). I Lincang Germanium Deposit, Southwest China; II Germanium Deposits of Russian Far East Region (1 Novikovsk; 2 Nizhne–Bikinsk; 3 Spetsugli; 4 Shkotovsk; Seredin, 2005); III Wulantuga Germanium Deposit, Inner Mongolia, North China.

and the input of dissolved REE and Y into the coal depositional sites, and the petrographic composition of coal is of secondary importance (fusain is enriched in REE and Y as compared to the whole coal samples from which they were selected) (Eskenazy, 1987a). Rare earth elements in coal appear to consist of a primary fraction,

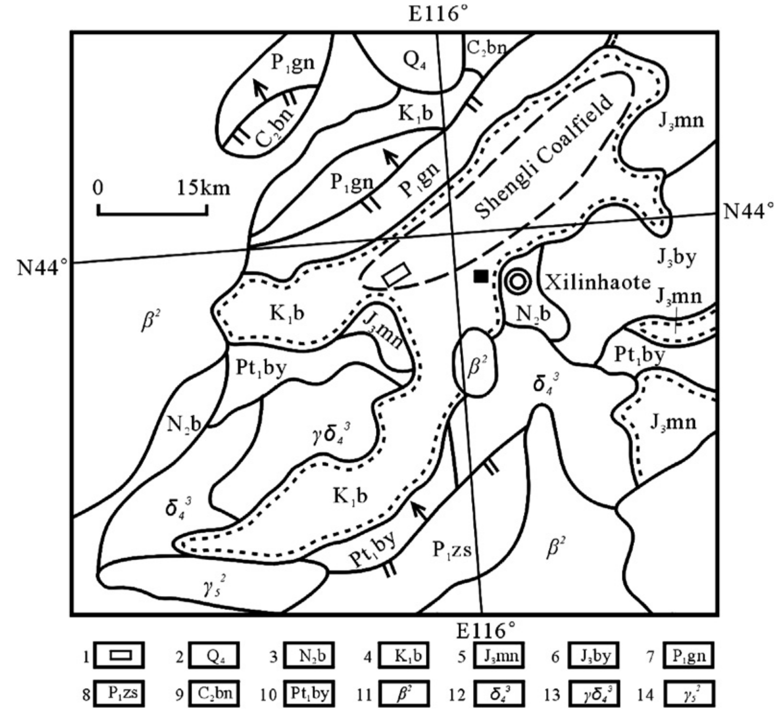

Fig. 2. The sketched regional geological map of Wulantuga Germanium Deposit (modified after Wang, 1999). 1. Wulantuga Germanium Deposit 2. Holocene 3. Neogene Baogedawula Group 4. Lower Cretaceous Bayanhua Group 5. Upper Jurassic Manitu Group 6. Upper Jurassic Baiyingaolao Group 7. Lower Permian Gegenaobao Group 8. Lower Permian Zhesi Group 9. Upper Carboniferous Benbatu Group 10. Lower Proterozoic Baoyintu Group 11. Quaternary Basalt 12. Hercynian Diorite 13. Hercynian Granodiorite 14. Late Jurassic Granite. The solid black square stands for Hongqi Coal Mine.

Table 1
With an exception of organic matter, semi-quantitative mineral composition (%) of low temperature (500 °C) ashes of lignite and sandstone samples from Shenli Coalfield as deduced from XRD analysis

	Qtz	Cal	Anh	Mm	K-feldspar	Ill	Plag	Iron mineral	Hm	Dol	Chl	Kao	Hbl	Gy
WL-1	28.6	53.1	3.7	4.5		7.5				Trace		2.7		
WL-3	4.4	86.3	6.3	2.5		0.6								
WL-5	54.5	28.0	6.1	4.6	6.9									
WL-13	7.5	85.0	7.5											
WL-17	8.4	78.3	9.4	3.8			Trace							
WL-25	25.1		16.9	10.0	8.4	27.8	5.0	6.9						
WL-27	45.4	41.3		2.6	2.6			4.3		3.9				
WL-30	53.3	6.7	18.0	2.4	10.8		Trace			6.3			2.4	
WL-31	39.1	6.9	43.4	4.7	6.0									
WL-33	26.3	2.9	15.8	4.9	4.6				40.1	Trace	5.7			
WL-36	40.3	41.0	2.2			5.6		9.7						1.2
WL-43	30.4	25.1	10.5		6.3	6.6	4.3	5.3		11.5				
WL-41[a]	70.7				12.8		16.5							
HQ-6[b]	27.2		27.2	6.4	9.6		8.0	17.5			4.2			
HQ-7[b]	40.0		11.6	6.6	3.8		19.4	9.1		7.6				

[a]Sandstone overlying the No. 6-1 coal seam; [b]Ge-barren lignites from Hongqi Coal Mine; The other samples are Ge-bearing lignite from WGD. Abbreviations of minerals (after Chace, 1956; Kretz, 1983): Qtz quartz; Cal calcite; Anh anhydrite; Mm montmorillonite; Ill illite; Plag plagioclase; Hm hematite; Dol dolomite; Chl chlorite; Kao kaolinite; Hbl hornblende; Gy gypsum.

which is associated with syngenetic mineral matter (Finkelman, 1982; Palmer et al., 1990). Another portion of the REE can be externally derived or mobilized when primary mineral matter is destroyed or modified, and may be retained in the coal bed but redistributed and incorporated into other mineral components (authigenic

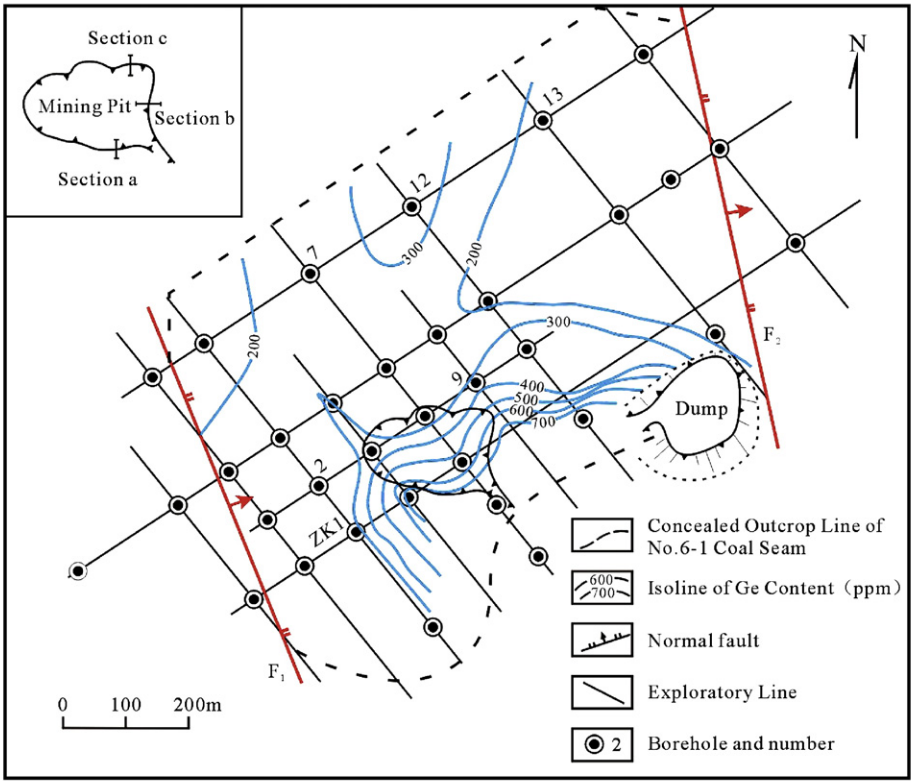

Fig. 3. Isopach map of Ge content in lignite from the Wulantuga Germanium Deposit (modified after Wang, 1999). The small fig on the top left corner show the spatial distribution of three sampling sections.

Table 2

Rare earth elements, Ge, TiO_2 concentrations (ppm) and ash yields (%) of lignites from the Wulantuga Germanium deposit (on whole coal dry basis)

	WL-1	WL-2	WL-3	WL-4	WL-5	WL-6	WL-7	WL-8	WL-9	WL-10	WL-11	WL-12	WL-13	WL-14	WL-15	WL-16	WL-17	WL-18	WL-19	WL-20	WL-21	WL-22	WL-23	WL-24	WL-25
La	42.0	13.0	5.94	27.6	47.3	17.6	18.7	7.01	7.26	5.70	5.56	6.80	3.71	9.07	5.13	9.55	5.96	9.18	5.31	6.08	5.71	1.66	2.29	7.73	10.6
Ce	57.8	24.5	10.3	48.5	105	30.9	35.0	13.8	14.8	10.7	10.2	11.7	7.07	17.4	8.94	17.7	11.5	18.2	10.4	11.8	12.2	3.59	4.47	17.0	21.8
Pr	6.13	2.81	1.13	5.55	13.7	3.37	3.80	1.62	1.61	1.13	1.11	1.30	0.84	1.93	1.01	1.94	1.24	2.05	1.17	1.34	1.38	0.42	0.54	2.19	2.71
Nd	23.9	10.3	4.38	21.4	58.5	12.6	13.9	6.19	5.83	4.17	3.95	4.80	3.43	7.26	3.91	7.12	4.40	7.45	4.31	4.94	4.89	1.69	2.21	8.78	11.0
Sm	4.10	1.82	0.82	3.54	11.6	2.06	2.32	1.21	1.08	0.75	0.64	0.78	0.66	1.32	0.70	1.27	0.81	1.42	0.80	0.83	0.78	0.35	0.41	1.93	2.30
Eu	0.89	0.24	0.14	0.60	2.23	0.35	0.43	0.24	0.19	0.12	0.14	0.16	0.13	0.22	0.13	0.21	0.15	0.24	0.15	0.12	0.16	0.07	0.08	0.40	0.46
Gd	5.04	1.78	0.86	3.56	11.4	2.05	2.30	1.20	1.04	0.77	0.63	0.82	0.74	1.24	0.72	1.29	0.81	1.34	0.76	0.87	0.83	0.35	0.42	1.70	2.01
Tb	0.78	0.27	0.13	0.47	1.63	0.28	0.31	0.17	0.15	0.11	0.09	0.11	0.11	0.18	0.10	0.21	0.12	0.20	0.12	0.11	0.12	0.06	0.06	0.29	0.34
Dy	4.85	1.64	0.72	2.62	9.36	1.63	1.85	0.99	0.84	0.63	0.54	0.68	0.67	1.07	0.61	1.26	0.73	1.07	0.73	0.60	0.71	0.34	0.32	1.85	2.01
Ho	1.02	0.34	0.14	0.53	1.96	0.32	0.37	0.19	0.15	0.11	0.10	0.13	0.14	0.21	0.12	0.26	0.13	0.20	0.14	0.13	0.14	0.06	0.07	0.35	0.38
Er	3.04	1.03	0.38	1.59	5.95	0.90	1.09	0.51	0.46	0.31	0.31	0.40	0.43	0.65	0.34	0.75	0.35	0.56	0.41	0.38	0.40	0.19	0.19	1.00	1.15
Tm	0.44	0.15	0.05	0.21	0.91	0.12	0.17	0.08	0.07	0.04	0.04	0.06	0.06	0.09	0.05	0.11	0.04	0.08	0.05	0.05	0.06	0.02	0.03	0.15	0.18
Yb	2.67	1.03	0.34	1.46	6.08	0.72	1.04	0.49	0.45	0.30	0.31	0.36	0.38	0.54	0.31	0.69	0.29	0.48	0.38	0.37	0.40	0.19	0.18	1.03	1.24
Lu	0.42	0.16	0.05	0.27	1.04	0.11	0.16	0.08	0.08	0.05	0.05	0.06	0.05	0.08	0.05	0.11	0.04	0.07	0.06	0.06	0.07	0.03	0.03	0.15	0.20
Y	35.6	9.40	4.54	19.6	55.1	10.6	11.3	5.39	4.66	3.30	2.95	4.76	5.71	6.60	4.06	7.99	4.17	5.57	4.18	2.93	3.13	1.83	2.01	7.52	9.25
∑REE	153	59.1	25.4	118	277	73.0	81.4	33.8	34.0	24.9	23.7	28.2	18.4	41.3	22.1	42.5	26.6	42.5	24.8	27.7	27.9	9.02	11.3	44.6	56.4
∑REE+Y	189	68.5	29.9	138	332	83.6	92.7	39.2	38.7	28.2	26.6	32.9	24.1	47.9	26.2	50.5	30.7	48.1	29.0	30.6	31.0	10.9	13.3	52.1	65.6
LREE	135	52.7	22.7	107	238	66.9	74.2	30.1	30.8	22.6	21.6	25.5	15.8	37.2	19.8	37.8	24.1	38.5	22.1	25.1	25.1	7.78	10.0	38.0	48.9
HREE	18.3	6.40	2.67	10.7	38.4	6.1	7.29	3.71	3.24	2.32	2.07	2.62	2.58	4.06	2.30	4.68	2.51	4.00	2.65	2.57	2.73	1.24	1.30	6.52	7.51
L/H	7.4	8.2	8.5	10.0	6.2	10.9	10.2	8.1	9.5	9.7	10.4	9.7	6.1	9.2	8.6	8.1	9.6	9.6	8.4	9.8	9.2	6.3	7.7	5.8	6.5
Eu/Eu*	0.59	0.40	0.51	0.51	0.59	0.52	0.57	0.60	0.54	0.48	0.67	0.61	0.56	0.52	0.56	0.50	0.56	0.53	0.58	0.43	0.60	0.61	0.59	0.67	0.65
Ge	133	31.4	53.4	288	179	30.9	52.8	41.9	68.5	88.6	152	672	1424	27.0	43.7	41.0	23.3	88.4	285	180	303	513	832	446	325
TiO_2	1681	1656	658	2923	3309	2405	3394	636	1181	340	863	731	298	1468	666	1747	834	905	675	853	633	210	280	895	1871
Ash	27.49	22.40	13.93	39.95	38.18	29.12	35.55	17.17	20.78	12.17	14.48	12.47	9.83	22.43	18.83	23.30	15.64	21.13	14.23	13.92	12.33	9.56	7.16	14.24	29.16

	WL-26	WL-27	WL-28	WL-29	WL-30	WL-31	WL-32	WL-33	WL-34	WL-35	WL-36	WL-37	WL-38	WL-39	WL-42	WL-43	WL-44	GM [a]	M_1 [a]	Min	Max	UCC [b]	USA [c]	WWC [d]
La	7.09	103	21.1	2.52	3.66	3.13	3.37	7.55	2.96	18.0	30.8	5.79	9.61	18.8	7.10	9.08	16.4	8.58	13.2	1.66	103	30	12	10
Ce	14.8	201	27.2	5.05	7.26	5.84	6.86	13.4	5.48	38.7	64.1	11.6	17.7	36.1	16.6	18.4	32.2	16.5	25.2	3.59	201	64	21	11.5
Pr	1.83	25.9	2.91	0.61	0.84	0.65	0.77	1.44	0.62	4.35	7.16	1.29	1.97	4.39	2.31	2.32	3.85	1.89	2.98	0.42	25.9	7.1	2.4	2.2
Nd	7.79	105	11.4	2.48	3.12	2.45	2.90	5.14	2.36	17.0	26.9	4.68	7.45	16.9	10.0	9.69	14.8	7.25	11.7	1.69	105	26	9.5	4.7
Sm	1.63	20.6	2.09	0.46	0.55	0.40	0.51	0.84	0.41	3.43	4.64	0.79	1.38	3.07	2.27	2.12	2.57	1.33	2.19	0.35	20.6	4.5	1.7	1.6
Eu	0.35	4.90	0.51	0.09	0.10	0.08	0.10	0.15	0.08	0.73	0.88	0.13	0.25	0.42	0.45	0.45	0.37	0.25	0.44	0.07	4.90	0.88	0.4	0.7
Gd	1.75	22.1	2.51	0.50	0.51	0.38	0.51	0.90	0.42	3.53	4.81	0.70	1.36	2.86	2.12	2.08	2.68	1.33	2.24	0.35	22.1	3.8	1.8	1.6
Tb	0.26	3.47	0.44	0.07	0.07	0.06	0.07	0.13	0.06	0.51	0.63	0.10	0.20	0.43	0.33	0.32	0.44	0.20	0.34	0.06	3.47	0.64	0.3	0.3
Dy	1.48	19.9	2.90	0.43	0.43	0.32	0.42	0.71	0.32	2.82	3.64	0.53	1.11	2.48	1.99	1.75	2.65	1.14	1.96	0.32	19.9	3.50	1.9	
Ho	0.30	3.92	0.62	0.08	0.09	0.06	0.08	0.15	0.06	0.52	0.73	0.11	0.2	0.52	0.39	0.34	0.58	0.23	0.39	0.06	3.92	0.80	0.35	0.3
Er	0.8	10.9	1.90	0.25	0.26	0.20	0.23	0.45	0.17	1.30	2.16	0.34	0.63	1.63	1.14	0.98	1.78	0.66	1.14	0.17	10.9	2.3	1	0.6
Tm	0.11	1.54	0.27	0.04	0.04	0.03	0.03	0.07	0.02	0.16	0.31	0.06	0.09	0.25	0.16	0.14	0.27	0.09	0.16	0.02	1.54	0.33	0.15	
Yb	0.69	9.09	1.64	0.27	0.26	0.21	0.20	0.41	0.15	0.97	2.09	0.47	0.57	1.63	1.01	0.92	1.75	0.62	1.05	0.15	9.09	2.20	0.95	0.5
Lu	0.12	1.39	0.27	0.04	0.04	0.03	0.03	0.07	0.03	0.14	0.33	0.08	0.09	0.26	0.16	0.15	0.27	0.10	0.17	0.03	1.39	0.32	0.14	0.07
Y	8.17	115	23.8	2.41	2.43	1.90	2.16	4.99	2.09	11.8	23.7	2.88	6.50	15.1	10.8	8.56	16.5	6.68	11.7	1.83	115	22	8.5	10
∑REE	39.0	533	75.8	12.9	17.2	13.8	16.1	31.4	13.1	92.2	149	26.7	42.6	89.7	46.0	48.7	80.6	40.3	63.2	9.02	533	146	53.6	34.1

∑REE+Y	47.2	648	99.6	15.3	19.7	15.7	18.2	36.4	15.2	104	173	29.6	49.1	105	56.8	57.3	97.1	47.2	74.9	10.9	648	168	62.1	44.1
LREE	33.5	460	65.2	11.2	15.5	12.6	14.5	28.5	11.9	82.2	134	24.3	38.4	79.7	38.7	42.1	70.2	35.9	55.7	7.78	460	132	47.0	30.7
HREE	5.51	72.3	10.6	1.68	1.70	1.29	1.57	2.89	1.23	9.95	14.7	2.39	4.25	10.1	7.30	6.68	10.4	4.39	7.45	1.23	72.3	13.9	6.59	3.37
L/H	6.1	6.4	6.2	6.7	9.1	9.7	9.2	9.9	9.7	8.3	9.1	10.2	9.0	7.9	5.3	6.3	6.7	8.17	8.32	5.31	10.9	9.5	7.1	9.1
Eu/Eu*	0.63	0.70	0.68	0.57	0.57	0.62	0.60	0.52	0.59	0.64	0.57	0.53	0.55	0.43	0.62	0.65	0.43	0.56	0.57	0.40	0.70	0.65	0.69	
Ge	872	133	78.5	329	517	432	164	254	339	1399	97.3	193	91.4	76.5	256	923	110	168	300	23.3	1424	1.6	5.7	5
TiO_2	250	2242	2187	188	923	532	522	646	167	1061	2618	607	950	2586	994	1752	1799	917	1218	167	3394	5000		300
Ash	11.30	29.83	29.05	10.87	13.13	10.95	6.86	12.65	8.43	23.21	23.58	14.08	20.46	30.33	13.41	15.79	25.88	17.15	18.93	6.86	39.95			

	CC[e]	M_1/UCC	M_1/US	M_1/WWA	M_1/CC	WL-40[f]	WL-41[f]	M_2[f]	HQ-2[g]	HQ-6[g]	HQ-7[g]	M_3[g]	M_1/M_2	M_1/M_3	SGD_H[h]	SGD_L[i]	LGD[j]	LUZ[k]
La	26.08	0.44	1.10	1.32	0.51	5.04	13.3	9.17	6.14	3.81	9.72	6.56	1.44	2.02	53.7	10.8	5.33	13.5
Ce	49.82	0.39	1.20	2.19	0.51	9.82	29.8	19.8	13	8.6	20.8	14.1	1.27	1.78	119	24.7	12.6	24.2
Pr		0.42	1.24	1.36		1.08	3.2	2.14	1.49	0.9	2.19	1.53	1.39	1.95	17.3		1.38	2.97
Nd	22.06	0.45	1.23	2.49	0.53	3.95	12.4	8.18	5.84	3.74	8.64	6.07	1.43	1.93	74.7	7.5	5.44	11.2
Sm	4.09	0.49	1.29	1.37	0.54	0.71	2.16	1.44	1.18	0.69	1.57	1.15	1.53	1.91	21.3	2.3	1.32	2.46
Eu	0.72	0.49	1.09	0.62	0.60	0.16	0.44	0.30	0.16	0.15	0.3	0.20	1.45	2.14	4.3	0.2	0.17	0.35
Gd		0.59	1.25	1.40		0.64	2.11	1.38	1.29	0.77	1.57	1.21	1.63	1.85	32.3		1.47	2.57
Tb	0.58	0.52	1.12	1.12	0.58	0.09	0.3	0.20	0.23	0.12	0.24	0.20	1.72	1.71	6.5	0.4	0.29	0.40
Dy		0.56	1.03			0.56	1.71	1.14	1.46	0.78	1.46	1.23	1.72	1.59	46.3		1.85	2.38
Ho		0.49	1.12	1.30		0.12	0.33	0.23	0.31	0.17	0.28	0.25	1.74	1.55	10.5		0.36	0.52
Er		0.50	1.14	1.90		0.36	0.95	0.66	0.9	0.47	0.82	0.73	1.74	1.56	31.7		1.08	1.49
Tm		0.50	1.10			0.05	0.14	0.10	0.13	0.07	0.12	0.11	1.73	1.54	4.7		0.17	0.22
Yb	1.78	0.48	1.10	2.10	0.59	0.37	0.87	0.62	0.84	0.45	0.79	0.69	1.69	1.51	30	1.9	1.27	1.46
Lu	0.52	0.52	1.20	2.39	0.32	0.06	0.13	0.10	0.14	0.07	0.12	0.11	1.76	1.52	4.6	0.2	0.21	0.22
Y		0.53	1.38	1.17		2.95	8.95	5.95	8.26	4.49	7.83	6.86	1.96	1.70	190	15.6	11.2	15.0
∑REE		0.43	1.18	1.85		23.0	67.8	45.4	33.1	20.8	48.6	34.2	1.39	1.85	457		33.0	63.9
∑REE+Y		0.44	1.21	1.70		26.0	76.8	51.4	41.4	25.3	56.5	41.0	1.46	1.82	647	63.6	44.2	78.9
LREE		0.42	1.19	1.82		20.8	61.3	41.0	27.8	17.9	43.2	29.6	1.36	1.88	290		26.3	54.6
HREE		0.54	1.13	2.21		2.25	6.54	4.40	5.30	2.90	5.40	4.53	1.70	1.64	167		6.71	9.26
L/H		0.87	1.17	0.91		9.2	9.4	9.3	5.2	6.2	8.0	6.5	0.90	1.29	1.9		5.0	6.1
Eu/Eu*						0.72	0.63	0.67	0.39	0.62	0.58	0.53			0.5		0.40	0.42
Ge		187	52.6	59.9		12.3	2.96	7.63	0.35	0.85	1.03	0.74	39.3	403		530	857	203
TiO_2		0.24		4.06		1199	2296	1748	769	590	1193	851	0.70	1.43			520	
Ash									11.69	9.00	14.31	11.67				25	13.47	23.4

WL-4 to WL-13 were collected from section a from the top downwards with an interval of 0.4–0.6 m; WL-14 to WL-26 were collected from section b from the top downwards with an interval of 0.5–0.6 m; WL-29 to WL-34 were collected from section c from the top downwards with an interval of 1.4 m. L/H = LREE/HREE.

[a]GM and M_1 represent the geometric mean and arithmetic mean of 42 lignite samples from WGD, respectively; [b]The average composition of upper continental crust (Taylor and McLennan, 1985); [c]The average composition of the USA coals (Finkelman, 1993); [d]The average composition of world wide coals (from Valkovic, 1983); [e]The average composition of the Chinese coals (Ren et al., 1999). [f]Sandstone samples collected from the overlying strata of No. 6-1 coal seam, M_2 stands for their arithmetic mean; [g]M_3 presents the arithmetic mean of three lignite samples collected from Hongqi Coal Mine; [h]SGD_H and [i]SGD_L represent the average composition of Ge-bearing coals from Spetsugli Germanium Deposit, Russia, with high and low REE contents, $n = 3$ and $n = 16$, respectively (Data after Seredin, 2005); [j]Arithmetic mean of 52 Ge-bearing lignites from LGD (Data after Qi et al., 2002b); [k]Arithmetic mean of 9 Ge-bearing lignites from Luzanovka, Russia (Data after Seredin et al., 2006).

Table 3
Correlation matrix of rare earth elements, Ge, TiO_2 concentrations and ash yields of the lignites from the Wulantuga Germanium Deposit ($n=38^{a}$, $p<0.05$)

	La	Ce	Pr	Nd	Sm	Eu	Gd	Tb	Dy	Ho	Er	Tm	Yb	Lu	Y	∑REE	∑REE+Y	LREE	HREE	L/H[b]	Ge	TiO_2	Ash
La	1.00	0.98	0.96	0.95	0.89	0.83	0.91	0.88	0.88	0.88	0.88	0.86	0.85	0.86	0.91	0.98	0.98	0.98	0.90	0.05	−0.15	0.88	0.92
Ce	0.98	1.00	0.99	0.99	0.94	0.87	0.95	0.91	0.89	0.89	0.88	0.85	0.85	0.85	0.86	1.00	0.99	1.00	0.91	0.04	−0.09	0.86	0.90
Pr	0.96	0.99	1.00	1.00	0.97	0.89	0.97	0.94	0.92	0.91	0.90	0.88	0.88	0.88	0.87	1.00	0.99	1.00	0.94	−0.03	−0.06	0.85	0.88
Nd	0.95	0.99	1.00	1.00	0.98	0.91	0.98	0.95	0.93	0.92	0.91	0.89	0.89	0.89	0.88	0.99	0.99	0.99	0.95	−0.09	−0.02	0.83	0.86
Sm	0.89	0.94	0.97	0.98	1.00	0.96	0.99	0.98	0.96	0.94	0.92	0.90	0.90	0.89	0.86	0.96	0.96	0.95	0.97	−0.22	0.05	0.77	0.80
Eu	0.83	0.87	0.89	0.91	0.96	1.00	0.96	0.96	0.95	0.92	0.88	0.85	0.84	0.83	0.84	0.89	0.90	0.88	0.93	−0.30	0.18	0.68	0.71
Gd	0.91	0.95	0.97	0.98	0.99	0.96	1.00	0.99	0.97	0.96	0.94	0.91	0.90	0.90	0.90	0.97	0.97	0.96	0.98	−0.22	0.07	0.76	0.80
Tb	0.88	0.91	0.94	0.95	0.98	0.96	0.99	1.00	0.99	0.99	0.97	0.95	0.94	0.93	0.92	0.94	0.95	0.93	0.99	−0.32	0.06	0.74	0.77
Dy	0.88	0.89	0.92	0.93	0.96	0.95	0.97	0.99	1.00	1.00	0.98	0.96	0.95	0.94	0.94	0.93	0.94	0.91	1.00	−0.35	0.03	0.74	0.77
Ho	0.88	0.89	0.91	0.92	0.94	0.92	0.96	0.99	1.00	1.00	0.99	0.98	0.97	0.96	0.96	0.92	0.94	0.91	1.00	−0.36	0.01	0.75	0.77
Er	0.88	0.88	0.90	0.91	0.92	0.88	0.94	0.97	0.98	0.99	1.00	0.99	0.99	0.98	0.97	0.91	0.94	0.90	0.99	−0.36	−0.04	0.77	0.78
Tm	0.86	0.85	0.88	0.89	0.90	0.85	0.91	0.95	0.96	0.98	0.99	1.00	1.00	0.99	0.95	0.89	0.91	0.87	0.97	−0.37	−0.08	0.78	0.77
Yb	0.85	0.85	0.88	0.89	0.90	0.84	0.90	0.94	0.95	0.97	0.99	1.00	1.00	0.99	0.93	0.89	0.91	0.87	0.97	−0.37	−0.09	0.77	0.77
Lu	0.86	0.85	0.88	0.89	0.89	0.83	0.90	0.93	0.94	0.96	0.98	0.99	0.99	1.00	0.94	0.89	0.91	0.87	0.96	−0.34	−0.10	0.78	0.78
Y	0.91	0.86	0.87	0.88	0.86	0.84	0.90	0.92	0.94	0.96	0.97	0.95	0.93	0.94	1.00	0.90	0.93	0.89	0.95	−0.28	−0.07	0.77	0.79
∑REE	0.98	1.00	1.00	0.99	0.96	0.89	0.97	0.94	0.93	0.92	0.91	0.89	0.89	0.89	0.90	1.00	1.00	1.00	0.95	−0.04	−0.07	0.86	0.89
∑REE+Y	0.98	0.99	0.99	0.99	0.96	0.90	0.97	0.95	0.94	0.94	0.94	0.91	0.91	0.91	0.93	1.00	1.00	0.99	0.96	−0.08	−0.07	0.85	0.89
LREE	0.98	1.00	1.00	0.99	0.95	0.88	0.96	0.93	0.91	0.91	0.90	0.87	0.87	0.87	0.89	1.00	0.99	1.00	0.93	0.00	−0.08	0.86	0.90
HREE	0.90	0.91	0.94	0.95	0.97	0.93	0.98	0.99	1.00	1.00	0.99	0.97	0.97	0.96	0.95	0.95	0.96	0.93	1.00	−0.32	0.01	0.77	0.79
L/H	0.05	0.04	−0.03	−0.09	−0.22	−0.30	−0.22	−0.32	−0.35	−0.36	−0.36	−0.37	−0.37	−0.34	−0.28	−0.04	−0.08	0.00	−0.32	1.00	−0.39	0.10	0.12
Ge	−0.15	−0.09	−0.06	−0.02	0.05	0.18	0.07	0.06	0.03	0.01	−0.04	−0.08	−0.09	−0.10	−0.07	−0.07	−0.07	−0.08	0.01	−0.39	1.00	−0.30	−0.33
TiO_2	0.88	0.86	0.85	0.83	0.77	0.68	0.76	0.74	0.74	0.75	0.77	0.78	0.77	0.78	0.77	0.86	0.85	0.86	0.77	0.10	−0.30	1.00	0.93
Ash	0.92	0.90	0.88	0.86	0.80	0.71	0.80	0.77	0.77	0.77	0.78	0.77	0.77	0.78	0.79	0.89	0.89	0.90	0.79	0.12	−0.33	0.93	1.00

[a]Except four samples (WL-1, WL-5, WL-27 and WL-36 in Table 2) with high REE contents. [b]L/H = LREE/HREE.

minerals)(Schatzel and Stewart, 2003). The superimposition of leachate of volcanic components or (hydrothermal) solution add to the enrichment of REE and Y in some coals, e.g., the highest concentration of Y plus the total rare earth elements (Y + ∑REE) in the Dean coal bed, Kentucky, is up to 2428 ppm (Seredin, 1996; Hower et al., 1999; Mardon and Hower, 2004; Seredin, 2005). This also leads the relative enrichment of heavy rare earth element (HREE) in some coals, when compared their REE composition to those of coal or shale in different stratum of a particular coal deposit (Seredin, 1996; Qi et al., 2002a,b; Schatzel and Stewart, 2003; Qi et al., 2004; Seredin, 2005). Therefore, the potential exists for using the REE as tracers to understand both the source and the epigenetic modification of coal mineral matter (Schatzel and Stewart, 2003).

As far as REE geochemistry of high-Ge coal is concerned, Qi et al. (2002a,b) found that Ge contents were negatively correlated with ratios of LREE/HREE, La_N/Yb_N, and Gd_N/Yb_N (N stands for chondrite normalization)

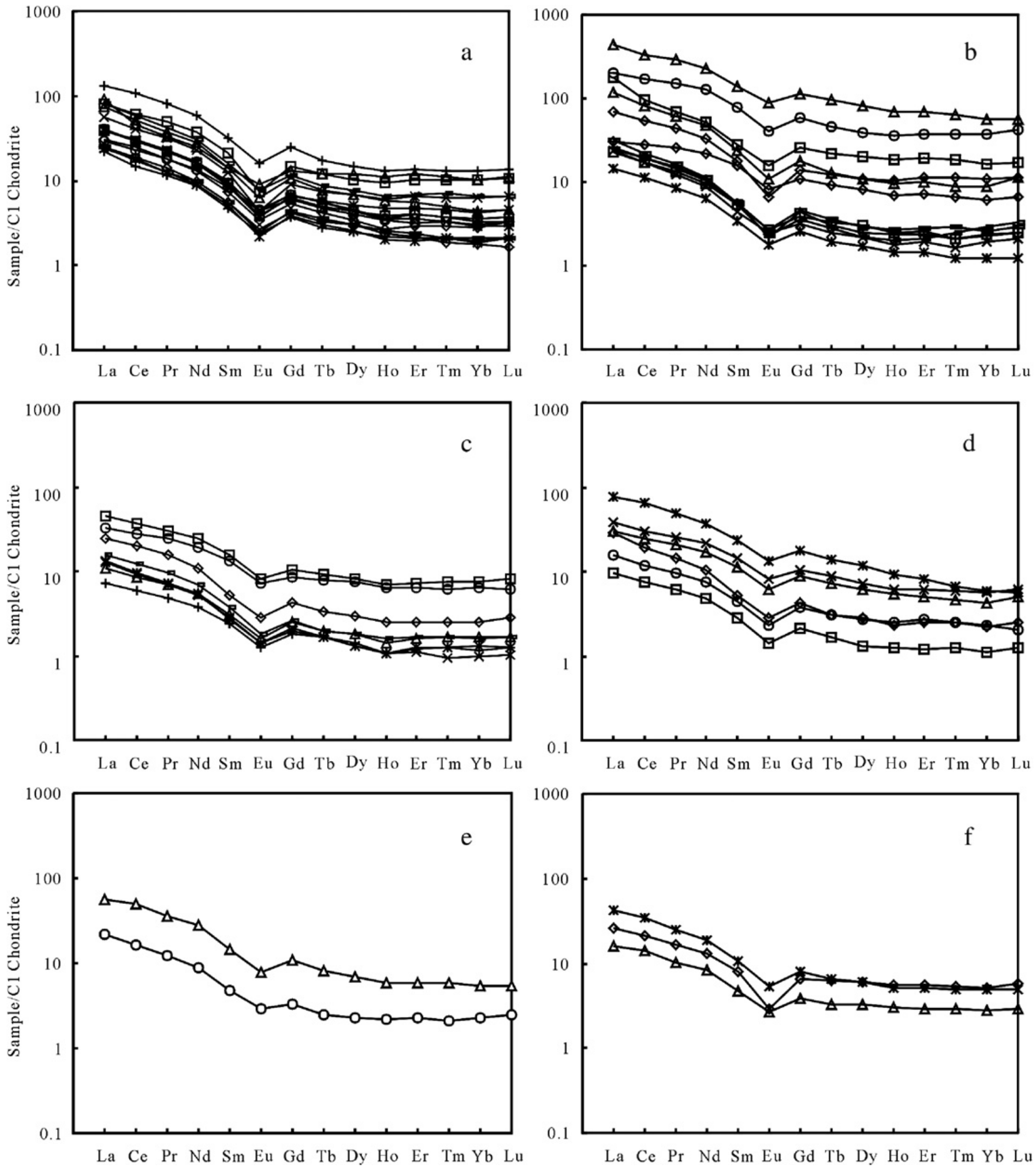

Fig. 4. C1 Chondrite-normalized REE patterns of different samples from WGD and Hongqi Coal Mine. a. Lignite samples with 23.3–97.3 ppm Ge; b. Lignite samples with 110–288 ppm Ge; c. Lignite samples with 303–517 ppm Ge; d. Lignite samples with 672–1424 ppm Ge; e. Sandstone samples from WGD; f. Lignite samples from Hongqi Coal Mine. Chondrite values after Anders and Grevesse (1989).

in the Ge-bearing coal of the Lincang Germanium Deposit (LGD), Yunnan, Southwestern China (Fig. 1). HREE is relatively enriched with increasing Ge content in these coals, when normalized to chondrite, North American Shale Composite (NASC) or the Ge-barren coal in the deposit area. REE patterns of the most Ge-enriched coals are similar to those of siliceous rocks which formed under hydrothermal environment (Qi et al., 2004). It was deduced that Ge and part of HREE in these coals were derived from a same hydrothermal source and were enriched in the coal during diagenesis (Qi et al., 2004), instead of the weathering of granite of basement as suggested by Zhuang et al. (1998).

Some Ge-bearing coals from Ge Deposits (such as Novikovsk, Shkotovsk, Spetsugli, and Nizhne–Bikinsk) of Russian Far East (GDRFE) (Fig. 1), especially the brown coals from the Spetsugli Germanium Deposit, show higher concentration (up to 1000 ppm on whole coal basis) of Y + ∑REE. When normalized to Ge-barren coal in the area, these

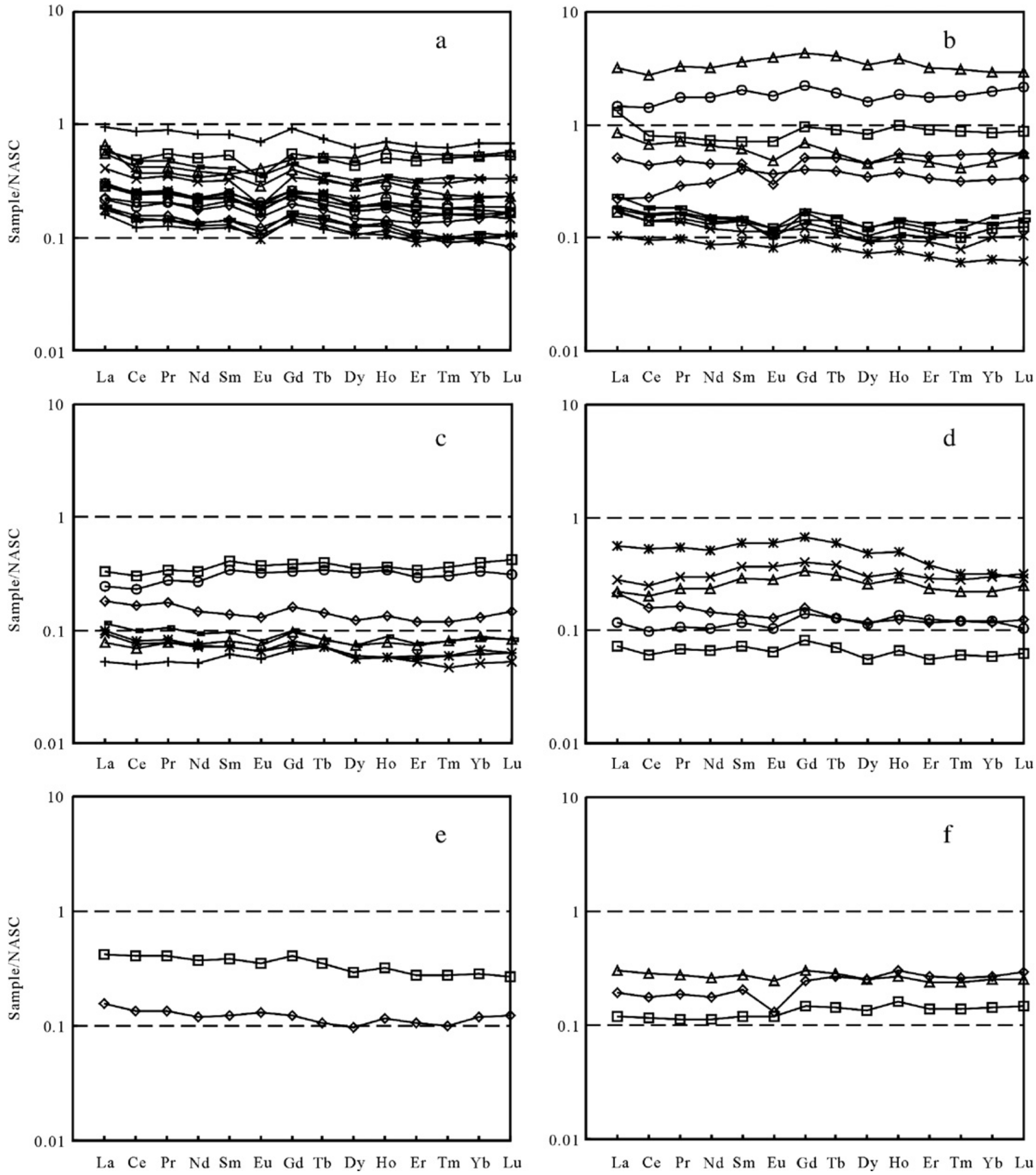

Fig. 5. NASC-normalized REE patterns of different samples from WGD and Hongqi Coal Mine. Symbols are the same as in Fig. 4. NASC values after Haskin et al. (1968).

Ge-bearing coals exhibit slight relative HREE enrichment. There is no distinct correlation between REE and Ge contents in these Ge-bearing coals. The enrichment of Y + ∑REE in these Ge-bearing coals was attributed to an epigenetic hydrothermal origin (Seredin, 1996, 2005).

The Wulantuga Germanium Deposit (WGD), the third largest Ge-bearing coal deposit area in the world, is located west of Xilinhaote, Inner Mongolia, Northeastern China (Fig. 1). The Ge contained in the deposit is estimated to be up to 1600 Mt, accounting for 30% of China's Ge reserves (Brown, 2000). Zhuang et al. (2006) reported REE contents of 12 coal samples from this deposit. However, the following questions still exist: (1) What is the major source of REE in these coals? (2) What is the mode of occurrence of REE in these coals? (3) What is the relationship between REE and Ge contents of these coals? (4) Is there any difference of REE geochemistry of Ge-bearing coals from different germanium deposits (LGD, SGD and WGD)? In this paper, we discussed the REE geochemistry of 42 lignite samples from WGD and addressed these questions specifically.

2. Geological setting

The Wulantuga Germanium Deposit is situated on the southwestern margin of Shengli Coalfield, limited to an area of 0.72 km^2 of the No. 6-1 coal seam (Fig. 2). The coalfield consists of monocline strata (Lower Cretaceous Bayanhua Formation) that dip 5–15° to north. The overlying strata consist mainly of sandstone and conglomerate, and the underlying strata consist mainly of dark mudstone, siltstone, and the unevenly distributed No. 6-2 coal seam (Du et al., 2003). The thickness of the No. 6-1 coal seam varies from 0.82 to 16.66 m, 9.88 m on average, and gradually increases from the outcrop of the No. 6-1 coal seam in the south part to the north part of mined area. The structure of this coal seam is quite simple, only one thin (0.15–0.30 m) carboniferous mudstone bench and five thin (<5 cm) clay partings occur in the lower and upper portions, respectively. This coal seam is characterized by a relatively high ash yield (21% db on average, $n=12$), relatively low calorific value (23.85 MJ/kg on average, $n=12$), sulfur content (1% db on average, $n=12$), high huminite (54–98%), low to medium inertinite (1–30%)

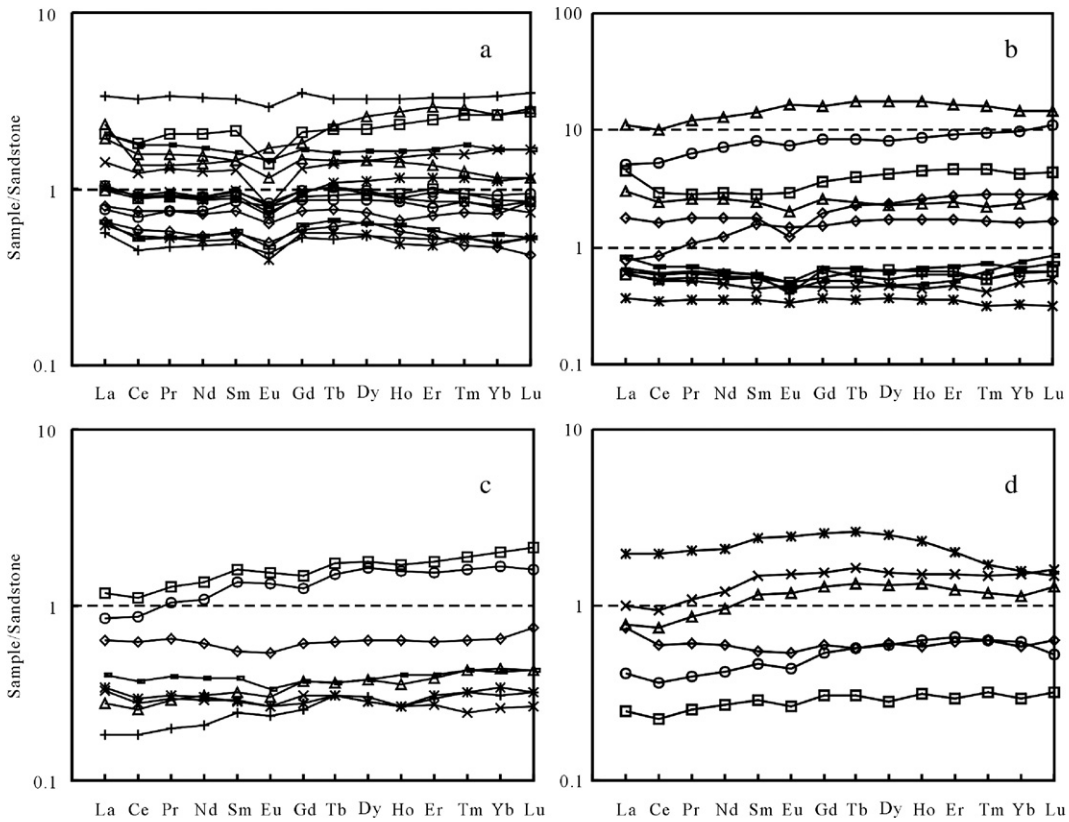

Fig. 6. Sandstone-normalized REE patterns of different lignite samples from WGD. Symbols are the same as in Fig. 4.

and liptinite (2–17.5%) contents (Zhuang et al., 2006). Mineral matter identified by XRD in low temperature ash (ashed at 500 °C in an open muffle) of lignite collected from this coal seam consists mainly of quartz, calcite, anhydrite, montmorillonite, and potassic feldspar (Table 1).

Ge mineralization occurs in the No. 6-1 coal seam. In the project controlled area, the southern and the northern extending part of the No. 6-1 coal seam contain relatively higher Ge than the eastern and western part (Fig. 3). In cross section, prospecting data show Ge content in the No. 6-1 coal seam ranges from 138 to 820 ppm, 244 ppm

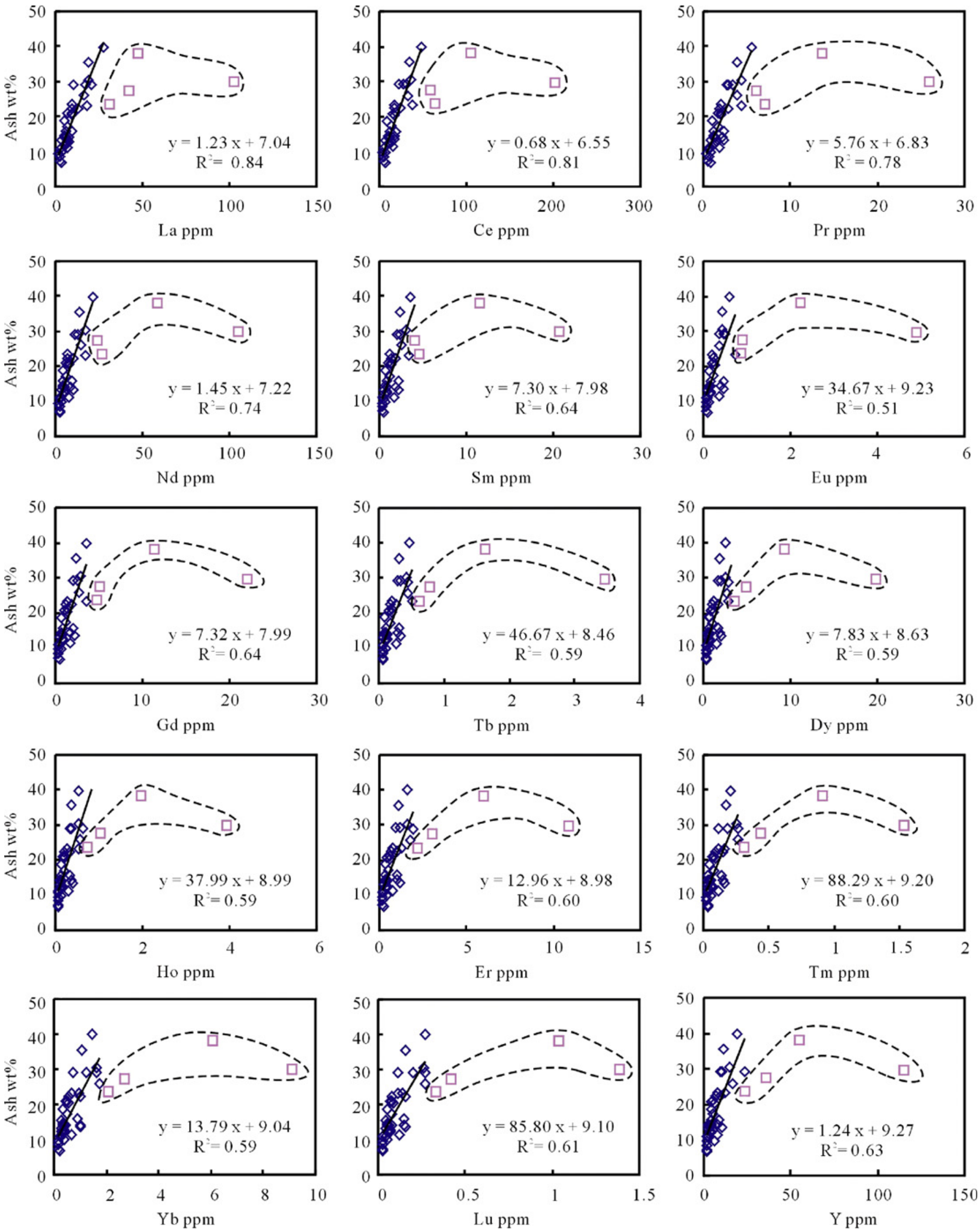

Fig. 7. Scatter diagram of ash yield against REE in lignite from WGD. The blank squares represent lignite samples with high content of ∑REE + Y, these sample were excluded when fitting the equation of trendline between ash yield and REE.

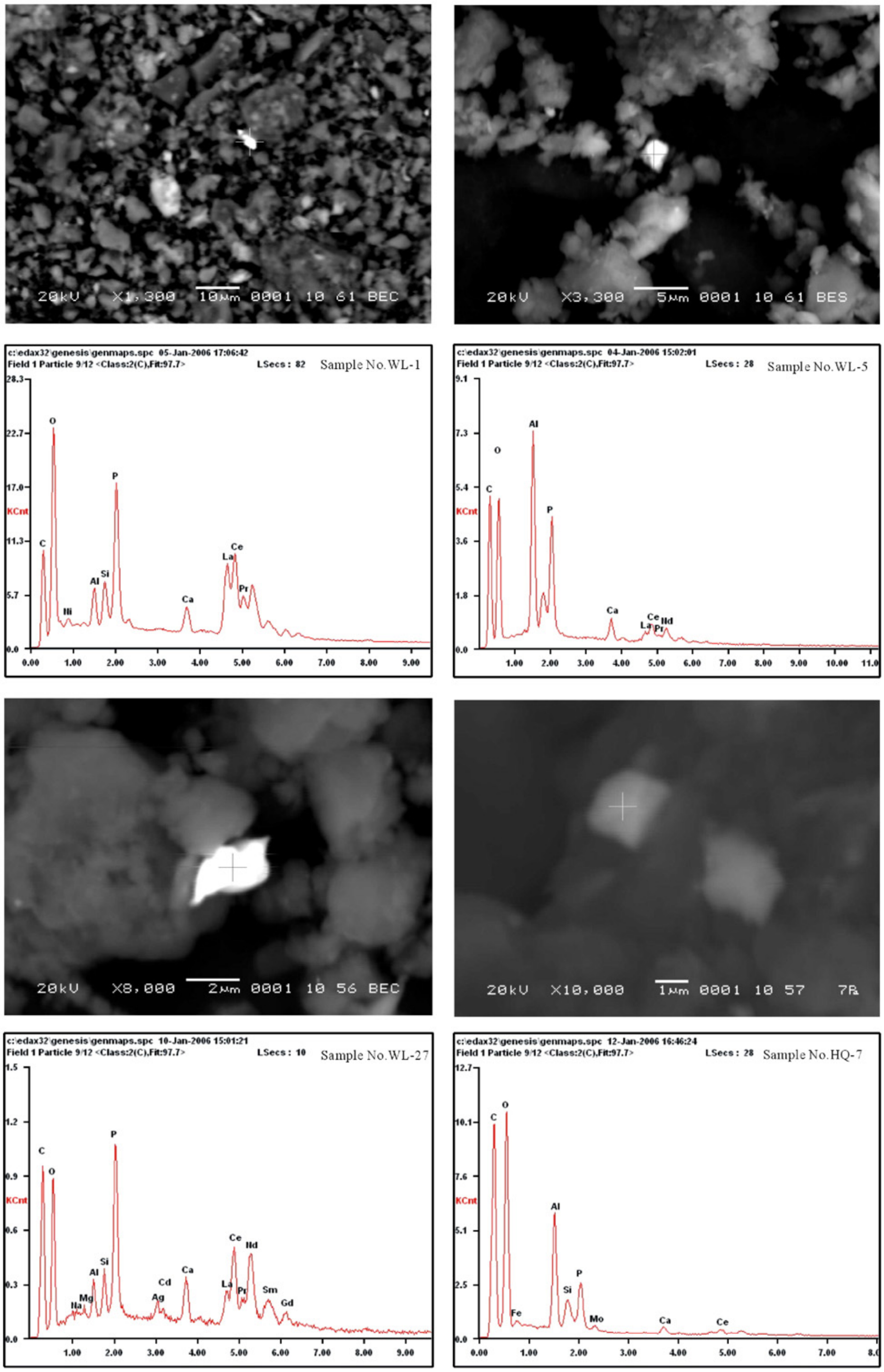

Fig. 8. Selected SEM microphotographs and EDX spectra of micron-sized monazite in the lignite from WGD and Hongqi Coal Mine.

on average (whole coal basis; Wang, 1999), and Ge enriched simultaneously in the top, bottom, and (or) the middle proportions of the No. 6-1 coal seam, depending on different locations of boreholes (Du et al., 2003). Most bore data show a peak of Ge content in the middle proportion of the No. 6-1 coal seam (Du et al., 2003). There are two faults, dipping 70–75° to NE and extending NNW along strike, in the western and eastern margin of the minefield (Fig. 3). These two faults interrupt the continuous distribution of the No. 6-1 coal seam. Detailed discussion of the geological setting of WGD and regional tectonic evolution can be found in Qi et al. (2007) and Zhuang et al. (2006).

3. Sampling and analytical methods

A total of 42 channel samples of lignite were collected from the recent strip-mine ledges of the No. 6-1 coal seam at different locations within the mine. Among the whole samples, 29 samples were sampled from the top downwards the coal seam at three different sections (section a, b and c in Fig. 3), with an interval of 20–100 cm, while the other samples were randomly collected from different parts of the coal seam. The bottom of the No. 6-1 coal seam is still unmined and buried, so no samples were collected from it. The sampling channel of each sample was 0.15-m wide, 0.20-m high, and 0.10-m deep. Two samples of sandstone from the overlying strata of the No. 6-1 coal seam in WGD minefield and three samples of lignite from the No. 6-1 coal seam in another mine without Ge mineralization, Hongqi Coal Mine, also were collected for comparison.

REE compositions of the all samples were determined by a PE Elan 6000 ICP-MS in Guangzhou Institute of Geochemistry, Chinese Academy of Sciences, following the method of Qi et al. (2007). Analytical errors were estimated to be less than 8% for most of REE. The modes of occurrence of REE in selected ground lignite samples were investigated by means of a JSM 6460 LV scanning electron microscope with energy-dispersive X-ray spectrometer (SEM-EDX) in the Institute of Geochemistry, Chinese Academy of Sciences. The organic/inorganic affinity of REE also were studied using the correlation of elements with 900 °C ash yields (Goodarzi, 1988; Foscolos et al., 1989; Krotenski and Sotirov, 2002).

4. Results and discussion

4.1. Contents of REE and Ge in lignite from WGD

The concentration of REE of 42 samples of lignite from WGD is presented in Table 2. The frequency distribution curves of REE and Y in all 42 samples are in accordance with the log normal distribution (Appendix 1), and their geometric means are distinctly lower than arithmetic means (Table 2). The content of ∑REE of

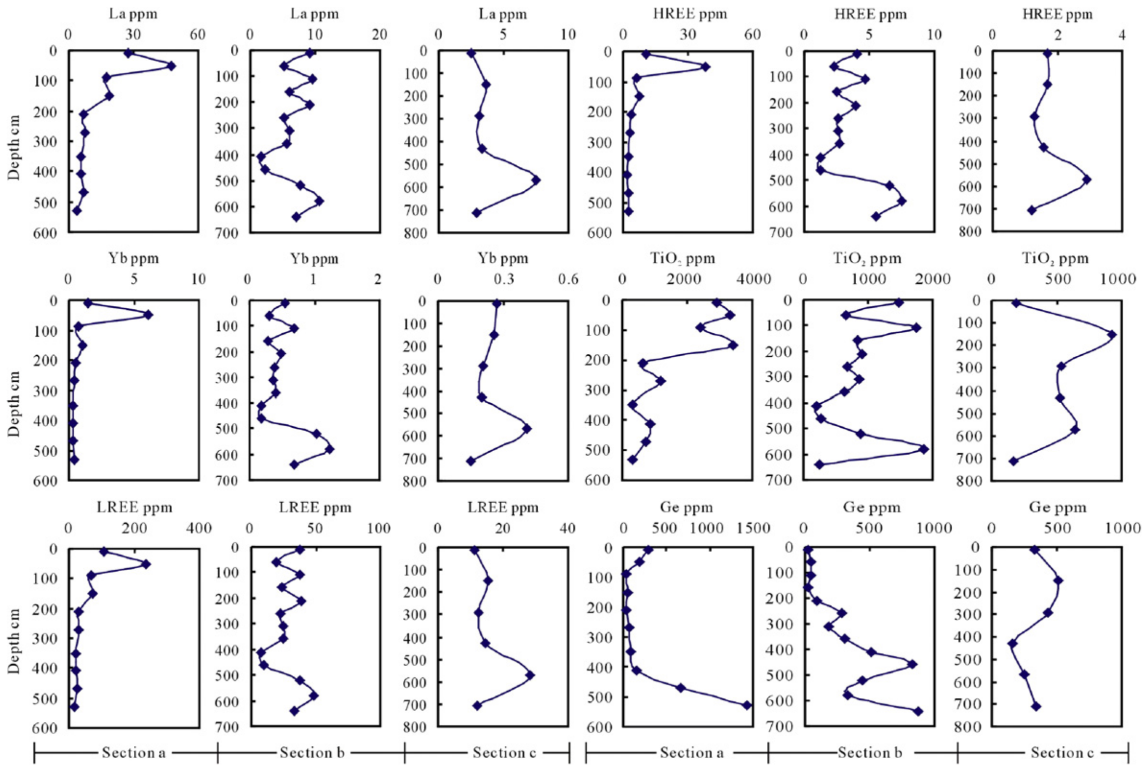

Fig. 9. Elemental concentration profiles of La, Yb, LREE, HREE, TiO_2, and Ge of lignite in three sections from WGD.

most lignite samples range from 9.02 to 118 ppm, only four samples show relatively higher (149–533 ppm) $\sum$REE concentration. The arithmetic means of REE and Y in the lignite from WGD are nearly half the average of composition of the Upper Continental Crust (Taylor and McLennan, 1985) and Chinese coals (Ren et al., 1999), but slightly higher than those of USA coals (Finkelman, 1993), world wide coals (Valkovic, 1983), sandstone from WGD, and Ge-barren lignite from Hongqi Coal Mine (Table 2). The Ge contents of 42 samples of lignite from WGD vary from 23.3 to 1424 ppm, 300 ppm on average. There is no distinct correlations between Ge and any individual REE or $\sum$REE + Y content of lignite from WGD (Table 3).

4.2. The REE patterns of lignite from WGD

The C1 chondrite-normalized REE patterns of lignite samples from WGD show commonly distinct negative Eu anomaly (the values of Eu/Eu* range from 0.40 to 0.70, 0.57 on average), and relative enrichment of LREE against HREE (ratios of LREE/HREE vary from 5.31 to 10.9, 8.32 on average), and generally are parallel to each other. These patterns are generally similar to those of the sandstone samples from WGD and Ge-barren lignite samples from Hongqi Coal Mine (Fig. 4). Especially, when normalized to NASC, these different lignites and sandstones from WGD and Hongqi Coal Mine generally show shale-like or flat REE patterns (Fig. 5), and a lower Eu anomaly (the values of Eu/Eu* range from 0.59 to 1.01, 0.82 on average) in comparison to the chondrite-normalized one, indicating REE of these different samples may have been derived from a similar terrigenous source and the Eu anomaly was inherited from the source rocks (Eskenazy, 1987b). When normalized to the average compositions of sandstone overburden, approximately three-quarters of total lignite samples from WGD show horizontal REE patterns, whereas a quarter of total samples display a small but distinct enrichment in middle-to heavy-REE (Fig. 6), indicating small quantity of middle-to heavy-REE may be added and/or retained during epigenesis (Schatzel and Stewart, 2003).

4.3. The mode of occurrence of REE

With an exception of four samples with high REE contents (Y + $\sum$REE range from 173 to 648 ppm), the

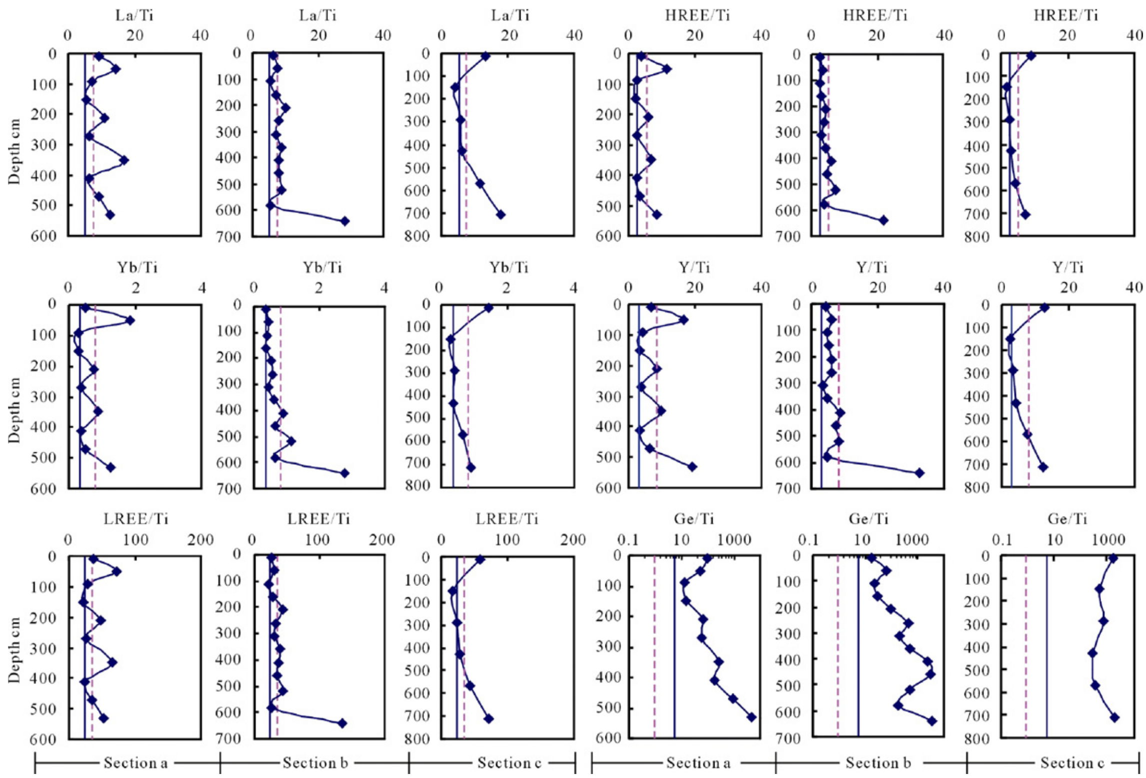

Fig. 10. TiO_2-normalized profiles of La, Yb, LREE, HREE, Y, and Ge of the lignite in three sections from WGD. Dashed line stands for the corresponding ratios of lignite from Hongqi Coal Mine, Solid line represents those of sandstone from WGD.

individual REE contents of 38 lignite samples from WGD are highly positively correlated with ash yields (Fig. 7). Their correlation coefficients ($r_{REE\text{-}Ash}$) range from 0.71 to 0.92 (Table 3), indicating a mainly detrital source and association with syngenetic mineral matter (Finkelman, 1982; Palmer et al., 1990). The enrichment of REE in four samples with high REE contents may be attributed to the existence of REE-rich phosphates (mainly monazite; see Birk and White, 1991), which were rarely identified by SEM-EDX in the lignite from WGD and Hongqi Coal Mine. These minerals generally occur as micron-size (2–5 μm) irregular grains (Fig. 8). Because it is stable in the weathering environment, monazite may be part of the heavy mineral fraction of the clastic sediments (Nesse, 2000). The irregular shapes of monazite in these medium-to high-ash (ash yields range from 23.58% to 38.18%) lignite samples, which close to top or mudstone interlayer, indicate that monazite may also derived from a detrital source.

4.4. Vertical profiles of REE and Ge

REE and Ge contents change both laterally and vertically. Representative vertical profiles of selective REE (La, Yb, LREE, and HREE) were compared to those of TiO_2 and Ge (Fig. 9) (more profiles of REE are included in Appendix 2). REE (La, Yb, LREE, and HREE) show coherent distributions in one special section, such as section a, b, or c, and mainly follow the distribution of TiO_2, concentrating in the upper and lower portions of different sections, distinctly distinguished from the vertical distribution of Ge. Although Ge also mainly concentrated in the upper and lower proportions of different sections, the positions where REE or Ge enriched in one special section are different. For example, REE is mainly concentrated in the upper proportion of section a, while Ge is mainly concentrated in the lower one (Fig. 9).

4.5. TiO_2-normalized profiles of REE and Ge

The contents of REE in the samples collected from three sections were normalized to TiO_2. The average values of corresponding ratios of the overlying sandstone from WGD and lignites from HCM were calculated as the reference guideline for comparison. The former may represent the background value of the input of detrital materials, and the latter may reflect the background value of various sources (detrital materials or solution) input during coal formation and later history without Ge mineralization (Qi et al., 2007). All these ratios were simplified as $element_i$/Ti and multiplied by 1000 for convenience of illustration in Fig. 10 and Appendix 3. Ratios of La/TiO_2, Yb/TiO_2, LREE/TiO_2, HREE/TiO_2, and Y/TiO_2 of lignite samples in three sections from WGD are greatly lower than those of Ge/TiO_2. These ratios fluctuate from top to bottom, and the lignite near top or bottom of the No. 6-1 coal seam show higher ratios than those of the lignite in the middle portion (Fig. 10). Generally, the average values of these ratios of all samples in one section is very close to that of the sandstone from WGD or lignite from HCM, indicate REE in the lignite of WGD mainly originated from detrital materials. More TiO_2-normalized profiles of REE are attached in Appendix 3.

4.6. Comparison with lignite from other Germanium deposits

When compared with the Ge-bearing lignite from LGD and GDRFE, the lignite samples from WGD show higher ratios of LREE/HREE and Eu/Eu* (Fig. 11), and there is no distinct correlation between Ge content and ratios of LREE/HREE (Table 3). The NASC-normalized REE patterns of lignite from WGD and the USA coals are horizontal ($La_{NS}/Yb_{NS}=1.22$, NS stands for NASC normalization), while those of Ge-bearing lignites from LGD and GDRFE are left-inclined or HREE relatively enriched (La_{NS}/Yb_{NS} range from 0.17

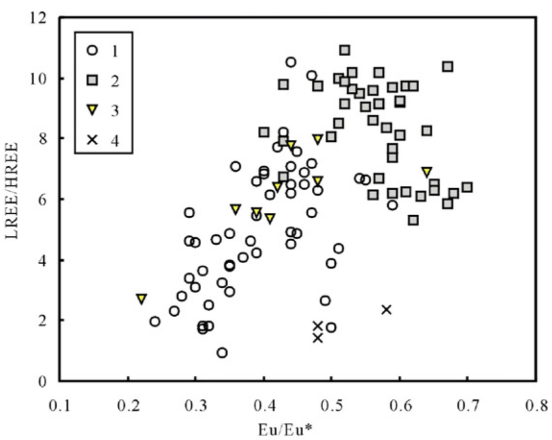

Fig. 11. Scatter diagram of LREE/HREE vs. Eu/Eu* of different Ge-bearing lignites. 1 Ge-bearing lignite from Lincang Germanium Deposit, Yunnan of China ($n=52$, on whole coal basis, Data after Qi et al., 2002b); 2 Ge-bearing lignite from Wulantuga Germanium Deposit, Inner Mongolia, China; 3 Ge-bearing lignite from Luzanovka Graben, Russian Far East (on whole coal basis, Data after Seredin et al., 2006); 4 Ge-bearing lignite with high content (398–811 ppm of ∑REE+Y from Spetsugli Germanium Deposit, Russian Far East (on whole coal basis, Data after Seredin, 2005).

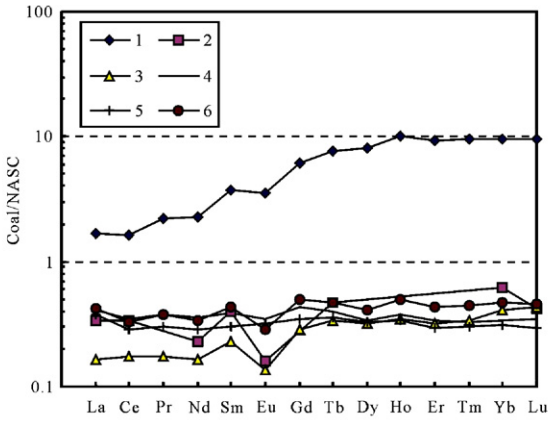

Fig. 12. NASC-normalized REE patterns of average composition of different coals. 1 The average composition of Ge-bearing lignite with high content of ∑REE+Y from Spetsugli Germanium Deposit, Russian Far East (n=3, on whole coal basis, Data after Seredin, 2005); 2 The average composition of Ge-bearing lignite with 33.2–95.4 ppm ∑REE+Y from Spetsugli Germanium Deposit, Russian Far East (n=16, on whole coal basis, Data after Seredin, 2005); 3 The average composition of Ge-bearing lignite from Lincang Germanium Deposit, Yunnan of China (n=52, on whole coal basis, Data after Qi et al., 2002b); 4 The average composition of the USA coals (Finkelman, 1993); 5 Ge-bearing lignite from Wulantuga Germanium Deposit, Inner Mongolia, China; 6 Ge-bearing lignite from Luzanovka Graben, Russian Far East (n=9, on whole coal basis, Data after Seredin et al., 2006).

to 0.90) (Fig. 12). The REE distribution in lignite from WGD belongs to N-type (LREE relatively enriched), while REE distributions in other Ge-bearing lignite belong to H-type (HREE relatively enriched) when compared with the average composition of the USA coals (Seredin, 2001). The different REE distribution in Ge-bearing lignite from WGD, LGD and GDRFE may be attributed to the difference of REE source. It is generally thought that the relatively enrichment of HREE in coal resulted from the interaction of coal with aqueous solutions (Seredin, 2001; Qi et al., 2002a,b; Schatzel and Stewart, 2003; Qi et al., 2004). As mentioned above, REE in the lignite from WGD mainly derived from a detrital source. The differences of REE and Ge geochemistry in the lignite from WGD imply that the genetic model (Ge might be enriched during epigenesis) of WGD may be different from those (Ge might be enriched during diagenesis) for LGD and GDRFE (Seredin, 1996; Hower et al., 2002; Yudovich, 2003; Qi et al., 2004; Seredin, 2005; Qi et al., 2007).

5. Conclusion

(1) The content of ∑REE of most lignite samples from WGD range from 9.02 to 118 ppm, only four samples show relatively higher (149–533 ppm) ∑REE concentration, which mainly caused by the existence of monazite as identified by SEM-EDX analysis. The average REE contents of 42 lignite samples from WGD are slightly higher than those of the USA coals, world wide coals, sandstone from WGD, and Ge-barren lignite from Hongqi Coal Mine.

(2) The lignite samples from WGD have shale-like Chondrite or NASC-normalized REE patterns similar to those of sandstone overburden and Ge-barren lignite from Hongqi Coal Mine; REE contents of most lignite samples are highly positively correlated with ash yields; The vertical profiles of REE mainly follow that of TiO_2, and the average element/TiO_2 ratios in three sections is very close to that of the sandstone from WGD or lignite from Hongqi Coal Mine. All these facts indicate a mainly detrital source and association with syngenetic mineral matter of REE in the lignite from WGD.

(3) When normalized to the overlying sandstone, some lignite samples from WGD display a small but distinct enrichment in middle-to heavy-REE, indicating small quantity of middle-to heavy-REE may be added and/or retained during epigenesis.

(4) The lignite samples from WGD are characterized by higher ratios of LREE/HREE and Eu/Eu*, and horizontal NASC-normalized REE patterns, and distinguished from those of the Ge-bearing lignites from LGD and GDRFE. There is no distinct correlations between Ge and any individual REE or ∑REE+Y content of lignite from WGD.

Acknowledgements

Natural Sciences Foundation of China financially supported this project (Grant No. 40302018 and Grant No. 40634020). The authors greatly acknowledge Tongli Ge Refine Co., Ltd., Xilingol, Inner Mongolia for their support during field sampling. We also appreciate Associate Professor Xianglin Tu in Guangzhou Institute of Geochemistry, Chinese Academy of Sciences, Engineer Jing Hu, Engineer Yurong Cai, and Associate Professor Xiuming Liu in the Institute of Geochemistry, Chinese Academy of Sciences, for the assistance during ICP-MS and SEM-EDX experiments. The suggestions of an unknown reviewer and James C. Hower (editor-in chief of this journal) largely improved the English of this Manuscript.

Appendix A. Supplementary data

Supplementary data associated with this article can be found, in the online version, at doi:10.1016/j.coal.2006.12.004.

References

Anders, E., Grevesse, N., 1989. Abundances of the elements: meteoritic and solar. Geochimica et Cosmochimica Acta 53, 197–214.

Birk, D., White, J.C., 1991. Rare earth elements in bituminous coals and underclays of the Sydney Basin, Nova Scotia: element sites, distribution, mineralogy. International Journal of Coal Geology 19, 219–251.

Brown, R.D., 2000. Germanium. U.S. Geological Survey Minerals Yearbook, 2000, pp. 33.1–33.3.

Chace, 1956. Abbreviations in field and mine geological mapping. Economic Geology 51, 712–723.

Du, G., Tang, D.Z., Wu, W., Sun, P.C., Bai, Y.L., Xuan, Y.Q., Huang, G.J., 2003. Preliminary discussion on genetic geochemistry of paragenetic Germanium Deposit in Shenli Coalfield, Inner Mongolia. Geoscience 17 (4), 453–458 (in Chinese with English abstract).

Eskenazy, G.M., 1987a. Rare earth elements and yttrium in lithotypes of Bulgarian coals. Organic Geochemistry 11, 83–89.

Eskenazy, G.M., 1987b. Rare earth elements in a sampled coal from the Pirin Deposit, Bulgaria. International Journal of Coal Geology 7, 301–314.

Finkelman, R.B., 1982. The origin occurrence, and distribution of the inorganic constituents in low rank coals. Proceedings of the Basic Coal Science Workshop. US Department of Energy, Houston, TX, pp. 69–90.

Finkelman, R.B., 1993. Trace and minor elements in coal. In: Engel, M.H., Macko, S. (Eds.), Organic Geochemistry. Plenum, New York, pp. 593–607.

Foscolos, A.E., Goodarzi, F., Koukouzas, C.N., Hatziyannis, G., 1989. Reconnaissance study of mineral matter and trace elements in Greek lignites. Chemical Geology 76, 107–130.

Goodarzi, F., 1988. Elemental distribution in coal seams at the fording coal mine, British Columbia, Canada. Chemical Geology 68, 129–154.

Haskin, L.A., Wilderman, T.R., Haskin, M.A., 1968. An accurate procedure for the determination of the rare earths by neutron activation. Journal of Radioanalytical and Nuclear Chemistry 1, 337–348.

Hower, J.C., Ruppert, L.F., Eble, C.F., 1999. Lanthanide, yttrium, and zirconium anomalies in the Fire Clay coal bed, Eastern Kentucky. International Journal of Coal Geology 39, 141–153.

Hower, J.C., Ruppert, L.F., Williams, D.A., 2002. Controls on boron and germanium distribution in the low-sulfur Amos coal bed, Western Kentucky coalfield, USA. International Journal of Coal Geology 53, 27–42.

Kretz, R., 1983. Symbols for rock-forming minerals. American Mineralogist 68, 277–279.

Krotenski, J., Sotirov, A., 2002. Trace and major element content and distribution in Neogene lignite from the Sofia Basin, Bulgaria. International Journal of Coal Geology 52, 63–82.

Mardon, S.M., Hower, J.C., 2004. Impact of coal properties on coal combustion by-product quality: examples from a Kentucky power plant. International Journal of Coal Geology 59, 153–169.

Nesse, W.D., 2000. Introduction to Mineralogy. Oxford University Press, Inc., New York, NY, pp. 349–350.

Palmer, C.A., Lyons, P.C., Brown, Z.A., Mee, J.S., 1990. The use of trace element concentrations in vitrinite concentrates and companion whole coals (hvA bituminous) to determine organic and inorganic associations. GSA Special Paper, vol. 248, pp. 55–62.

Qi, H.W., Hu, R.Z., Su, W.C., 2002a. REE geochemistry of Lignites in the Lincang germanium deposit, Western Yunnan Province, China. Goldschmidt Conference Abstracts, p. A619.

Qi, H.W., Hu, R.Z., Su, W.C., Qi, L., 2002b. REE geochemistry of lignites in Lincang Germanium Deposits, Yunnan Province. Geochimica 31, 300–308 (in Chinese with English abstract).

Qi, H.W., Hu, R.Z., Su, W.C., Qi, L., Feng, J.Y., 2004. Continental hydrothermal sedimentary siliceous rock and genesis of superlarge germanium (Ge) deposit hosted in coal: a study from the Lincang Ge deposit, Yunnan, China. Science in China, Series D: Earth Sciences 47, 973–984.

Qi, H.W., Hu, R.Z., Zhang, Qi., 2007. Concentration and distribution of trace elements in Lignite from the Shengli Coalfield, Inner Mongolia, China: Implications on origin of the associated Wulantuga Germanium Deposit. International Journal of Coal Geology 71, 129–152. doi:10.1016/j.coal.2006.08.005.

Ren, D.Y., Zhao, F.H., Wang, Y.Q., Yang, S.L., 1999. Distributions of minor and trace elements in Chinese coals. International Journal of Coal Geology 40, 109–118.

Schatzel, S.J., Stewart, B.W., 2003. Rare earth element sources and modification in the Lower Kittanning coal bed, Pennsylvania: implication for the origin of coal mineral matter and rare earth element exposure in underground mines. International Journal of Coal Geology 54, 223–251.

Seredin, V.V., 1996. Rare earth element-bearing coals from the Russian Far East deposits. International Journal of Coal Geology 30, 101–129.

Seredin, V.V., 2001. Major regularities of the REE distribution in coal. Doklady Earth Sciences 377, 250–253.

Seredin, V.V., 2005. Rare earth elements in germanium-bearing coal seams of the Spetsugli Deposit (Primor'e Region, Russia). Geology of Ore Deposits 47, 238–255.

Seredin, V.V., Danicheva, Y.A., Magazina, L.O., Sharova, I.G., 2006. Ge-bearing coals of the Luzanovka Graben, Pavlovka Brown Coal Deposit, Southern Primorye. Lithology and Mineral Resources 41, 280–301.

Taylor, S.R., McLennan, S.M., 1985. The continental crust: its composition and evolution. Blackwell scientific publications, Oxford, pp. 9–67.

Valkovic, V., 1983. Trace Elements in Coal, vol. 1. CRC Press, pp. 133–138.

Wang, L.M., 1999. Introduction of the geological feature and explorating of Wulantuga germanium deposit in Xilinguole League, Inner Mongolia. Geology of Inner Mongolia 3, 15–20 (in Chinese with English abstract).

Yudovich, Y.E., 2003. Notes on the marginal enrichment of Germanium in coal beds. International Journal of Coal Geology 56, 223–232.

Zhuang, H.P., Lu, J.L., Fu, J.M., Liu, J.Z., 1998. Lincang superlarge germanium deposit in Yunnan province, China: sedimentation, diagenesis, hydrothermal process and mineralization. Journal of China University of Geosciences 9, 129–136.

Zhuang, X.G., Querol, X., Alastuey, A., Juan, R., Plana, F., Soler, A.L., Du, G., Martynov, V.V., 2006. Geochemistry and mineralogy of the Cretaceous Wulantuga high-Germanium coal deposit in Shengli coal field, Inner Mongolia, Northeastern China. International Journal of Coal Geology 66, 119–136.